Multicarrier M-ary Orthogonal Chaotic Vector Shift Keying with Index Modulation for High Data Rate Transmission

Xiangming Cai, Weikai Xu, *Member, IEEE,* Lin Wang, *Senior Member, IEEE,* G. Kolumbán, *Fellow, IEEE*

***Abstract*—A new multicarrier M-ary orthogonal chaotic vector shift keying with index modulation (MC-MOCVSK-IM) is presented in this paper. In this design, information bits are conveyed not only by the multiple groups of M-ary information bearing signals, but also by the specific indices of the selected reference signals which depend on the incoming mapped bits. Benefiting from the favorable features of multicarrier modulation, M-ary modulation and index modulation, MC-MOCVSK-IM system is capable to offer higher energy efficiency and spectral efficiency at some expense of hardware complexity. In addition, the analytical bit error rate (BER) expressions of MC-MOCVSK-IM system are derived over additive white Gaussian noise (AWGN) and multipath Rayleigh fading channels. The BER performance comparison between MC-MOCVSK-IM system and other non-coherent chaotic communication systems is carried out to highlight the superiority of MC-MOCVSK-IM system in terms of BER performance. Considering the dramatically increased demand for high-data-rate transmission and the harsh environment of future wireless communication, MC-MOCVSK-IM system shows strong robustness and offers competitive solutions for high-data-rate non-coherent chaotic communication systems.**

***Index Terms*—Chaotic communication, orthogonal chaotic vector shift keying (OCVSK), multicarrier modulation, M-ary modulation, index modulation, high data rate.**

I. Introduction

The significant driving force in advanced wireless communications is the promise of high-rate-data transmission. In this perspective, the explosive growth of mobile applications as well as the thirsty demand for high data rate urges researchers and engineers to design high-data-rate-oriented and reliable wireless communication systems which are capable of coping with frequency-selective fading wireless channel. However, symbol duration is reduced with the increasing data rate, and the scattered fading of wireless channels will cause more severe inter-symbol interference (ISI) if single-carrier modulation is used [1]. Therefore, multicarrier technique emerges in this context and it has been extensively used for broadband wireless communications [2]. Multicarrier modulation decomposes the data stream into several parallel substreams where the symbol period becomes longer, therefore multicarrier systems show better robustness against frequency-selective fading channels when the bandwidth of each subcarrier is much less than coherent bandwidth.

Chaotic signals are originated from the nonlinear dynamical systems [3], characterized by broadband, noise-like and non-period properties. In addition, chaotic signals possess a special property, known as *sensitive dependence upon initial conditions* [4]. Motivated by the excellent characteristics of chaotic signals, many researchers have applied chaotic signals to the design of spread-spectrum (SS) communication systems [5]–[8]. Since non-coherent differential chaos shift keying (DCSK) was proposed by Kolumbán *et al.* in [6], many variants of DCSK have been designed over the last two decades, mainly exploiting their capability of offering reliable performance in multipath fading channel. Besides, neither chaos synchronization nor channel state information (CSI) is needed in DCSK system [9]. However, DCSK system inevitably has the problem of energy loss because of its transmitted-reference structure. Explicitly, half symbol period of DCSK system is used to transmit non-information-bearing reference signal, causing inferior energy efficiency and low data rate.

Considering the exponential growth of wireless applications and the continuous increase in the requirement of high-data-rate service, many researchers began to design high-throughput chaotic communication systems. The representative schemes are quadrature chaos shift keying (QCSK) [10] and its generalized M-ary version [11], namely the M-ary DCSK system. In M-ary DCSK system, high-data-rate goal is achieved by modulating multiple information bits into M-ary constellation symbol. In [12], the generalized code-shifted DCSK (GCS-DCSK) separates reference and multiple information bearing signals via different Walsh code sequences and then the resultant signal is transmitted within the identical time slot. Consequently, it improves spectral efficiency and eliminates the need for delay lines simultaneously [13]. By using different chaotic sequences rather than limited Walsh code sequences to separate reference and information bearing signals, a high-data-rate code-shifted DCSK (HCS-DCSK) [14] can offer high data rate and strengthen data security. The promising code-shifted idea has become a hot research topic and many researchers proposed new non-coherent chaotic communication systems including multilevel code-shifted DCSK (MCS-DCSK) [15] and its M-ary version MCS-MDCSK [16].

In addition, multicarrier modulation technique provides another perspective to improve the data rate. By integrating

Xiangming Cai, Weikai Xu and Lin Wang are with the Department of Information and Communication Engineering, Xiamen University, Xiamen, P. R. China. (e-mail: samson0102@qq.com, xweikai@xmu.edu.cn, wanglin@xmu.edu.cn).

G. Kolumbán is with the Faculty of Information Technology and Bionics, Pázmány Péter Catholic University, Budapest, Hungary (e-mail: kolumban@itk.ppke.hu) and he is an Adjunct Prof. at the School of Engineering, Edith Cowan University, Perth, Australia.

This work was supported by the National Natural Science Foundation of China under Grant No. 61671395 and 61871337.

multicarrier modulation into DCSK system, Kaddoum *et al.* proposed a non-coherent multicarrier DCSK (MC-DCSK) system where a chaotic reference signal is transmitted over a predefined subcarrier frequency and multiple information data streams are transmitted over the remaining subcarriers [17]. In that configuration, the data rate as well as spectral efficiency is improved without the penalty on BER performance. Due to the excellent feature of orthogonal frequency division multiplexing (OFDM) technique, the author of [18] has proposed a multiuser OFDM-based DCSK (MU OFDM-DCSK) in which IFFT/FFT operations rather than parallel matched filters used in MC-DCSK system are employed to get a low complexity.

Recently, index modulation (IM) [19] has become a promising technique, whereby the specific indices of different transmission entities, including spreading codes, time slots and subcarriers, are used to carry extra information bits and therefore, it creates a completely new dimension for data transmission. There is currently a strong interest in extending IM technique to the field of chaotic communications. The promising idea of integrating index modulation into multicarrier chaotic modulation schemes has been elaborated by Cheng *et al.* and carrier index DCSK (CI-DCSK) as well as its M-ary modulation scheme (CI-MDCSK) has been proposed in [20] and [21], respectively. Other researchers have proposed a two-layer carrier index DCSK (2CI-DCSK) system which reuses subcarrier resources, and thus higher data rate and spectral efficiency are obtained at the expense of slightly larger complexity [22]. More recently, dual-index modulation has been introduced into chaotic communications and Cai *et al.* proposed a non-coherent DCSK with dual-index modulation (DCSK-DIM) where two parallel time slot indices are served as a new dimension for information transmission [23]. CIM-MC-M-DCSK system was proposed in [24] to obtain higher data rate and better BER performance where code index modulation and M-DCSK modulation are applied for reference signals and information-bearing signals, respectively.

Orthogonal chaotic vector shift keying (OCVSK) [25] is another beneficial chaotic modulation scheme for the purpose of higher data rate. To address the limitation of data rate in OCVSK system, Hasan *et al.* applied OFDM technique to OCVSK system and then proposed a hybrid modulation scheme referred to as OFDM-OCVSK [26]. By combining multicarrier transmission and multilevel chaotic shift keying modulation, a non-coherent multicarrier chaotic shift keying (MC-CSK) system was designed in [27]. Radically, MC-CSK system can be subsumed under OCVSK-based multicarrier modulation schemes. In MC-CSK system, physical information bits are not directly transmitted by multicarrier symbols but by the specific indices of reference subcarriers. Although the data rate and spectral efficiency of MC-CSK system can be enhanced to some extent, there is still tremendous margin for improvement if multicarrier symbols are also applied to carry information bits.

Although CI-DCSK and 2CI-DCSK systems can achieve superior BER performance, their energy efficiency and spectral efficiency are unsatisfactory. Because only one subcarrier is activated for information bearing signal in CI-DCSK system and two subcarriers are applied to carry information bearing signal in 2CI-DCSK system. Therefore, lots of subcarriers are not used for information transmission and this results in great waste of subcarrier resource. MC-DCSK and MC-CSK make full use of subcarriers, however their BER performances are not good. Considering the constraint of CI-DCSK, 2CI-DCSK, MC-DCSK and MC-CSK systems, we present a new non-coherent multicarrier M-ary orthogonal chaotic vector shift keying with index modulation (MC-MOCVSK-IM) to achieve better energy efficiency, higher spectral efficiency and preferable BER performance. In this design, information bits are transmitted not only by the M-ary constellation symbols, but also by the specific indices of the selected reference signals. The main contributions of this paper are as follow:

- A new multicarrier M-ary orthogonal chaotic vector shift keying scheme with index modulation is proposed. Its energy efficiency, spectral efficiency and system complexity are analyzed. Compared to CI-DCSK and 2CI-DCSK systems, MC-MOCVSK-IM system is capable to achieve higher energy efficiency and excellent spectral efficiency at the expense of system complexity.
- We analyse the bit error probability of MC-MOCVSK-IM over AWGN and multipath Rayleigh fading channels. Then, the validity of analytical results is verified by computer simulations.
- The BER performance comparisons of MC-MOCVSK-IM and its competitors for the case of same number of transmitted bits per symbol and same number of subcarriers are performed. The results of comparison demonstrate that MC-MOCVSK-IM can obtain better BER performance than its competitors.

The remainder of this paper is organized as follows. Section II describes MC-MOCVSK-IM system model in detail. System analysis is presented in Section III, while Section IV gives the performance analysis of the proposed system. The simulation results are presented in Section V. Conclusions are drawn in Section VI.

II. System Model

A. The Transmitter

The block diagram of MC-MOCVSK-IM transmitter is shown in Fig. 1. First, by utilizing the excellent property of chaotic signal, namely sensitive dependence upon initial conditions, several β-length chaotic signals are generated by a logistic map $c_{j+1} = 1 - 2c_j^2$, $j = 0, 1, 2, \cdots$ with different initial values. In particular, the N chaotic signals are uncorrelated with each other [4]. Define a β rows and N columns matrix as $\mathbf{C}_{\beta\times N} = [\mathbf{c}_1, \mathbf{c}_2, \cdots, \mathbf{c}_N]$ where the column vector $\mathbf{c}_j = [c_{1,j}, c_{2,j}, \cdots, c_{\beta,j}]^{\mathrm{T}}$ is generated by the j^{th} chaotic signal generator and $[\cdot]^{\mathrm{T}}$ is transposition operation. Mathematically, $c_{i,j}$ denotes i row and j column of matrix $\mathbf{C}_{\beta\times N}$, while $\mathbf{c}_j$ represents the column vector in matrix $\mathbf{C}_{\beta\times N}$. Apparently the matrix $\mathbf{C}_{\beta\times N}$ is column full rank and thus the rank of $\mathbf{C}_{\beta\times N}$ is equal to N when $\beta \geq N$. Therefore, the condition of linear independence for Gram-Schmidt algorithm is satisfied. Then, Gram-Schmidt algorithm is applied to obtain orthogonal and normalized chaotic signals,

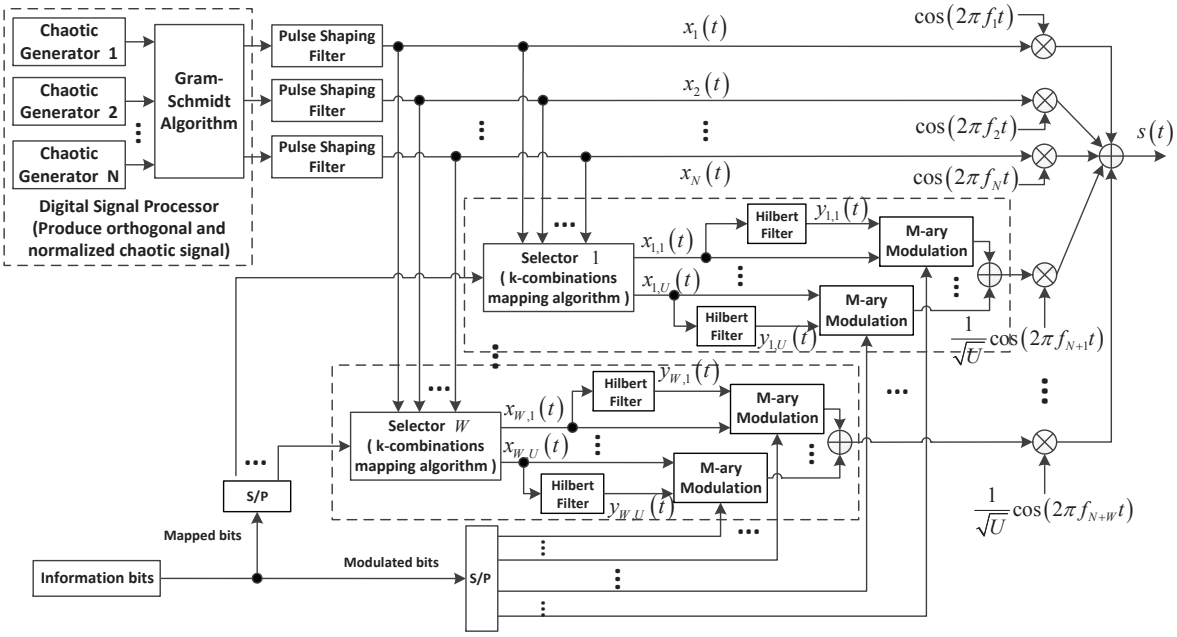

Fig. 1. The block diagram of MC-MOCVSK-IM transmitter.

described as [27], [28]

$$\mathbf{e}_j = \begin{cases} \frac{\mathbf{c}_1}{\|\mathbf{c}_1\|_2}, & j = 1, \\ \frac{\mathbf{c}_j - \sum_{k=1}^{j-1} \frac{\langle \mathbf{c}_j, \mathbf{e}_k \rangle}{\langle \mathbf{e}_k, \mathbf{e}_k \rangle} \mathbf{e}_k}{\left\| \mathbf{c}_j - \sum_{k=1}^{j-1} \frac{\langle \mathbf{c}_j, \mathbf{e}_k \rangle}{\langle \mathbf{e}_k, \mathbf{e}_k \rangle} \mathbf{e}_k \right\|_2}, & j = 2, 3, \cdots, N, \end{cases} \tag{1}$$

where $\|\mathbf{c}_1\|_2$ represents 2-norm of vector $\mathbf{c}_1$, given as $\|\mathbf{c}_1\|_2 = \sqrt{\sum_{j=1}^{\beta} |c_{j,1}|^2}$. Besides, $\langle \mathbf{c}_j, \mathbf{e}_k \rangle = \sum_{i=1}^{\beta} c_{i,j} (e_{i,k})^*$ is the inner product of vectors $\mathbf{c}_j$ and $\mathbf{e}_k$ where $(\cdot)^*$ denotes conjugate operation. The outputs of Gram-Schmidt Algorithm is a matrix, i.e., a collection of chaotic sequences. These chaotic sequences are converted into analog signals by a square root raised-cosine pulse shaping filter. At the outputs of pulse shaping filters, N orthogonal and normalized reference chaotic signals are obtained as

$$x_j(t) = \sum_{i=1}^{\beta} e_{i,j} h_p(t - iT_c), \quad j = 1, 2, \cdots, N \tag{2}$$

where β is spreading factor and T_c is the interval of chaotic samples. $e_{i,j}$ denotes the i^{th} sample of the j^{th} normalized chaotic signal and $h_p(t)$ represents the normalized impulse response of square root raised-cosine filter with roll-off factor α, $0 < \alpha \leq 1$.

As shown in Fig. 1, there are N chaotic signals modulated by N different subcarriers as reference signals. Simultaneously, W groups information bearing signals are transmitted by other subcarriers in a parallel manner. It should be noted that there are U information bearing signals modulated by M-ary constellation symbols in each group. The reference signals corresponding to these U information bearing signals are selected from the N different reference signals via k-combinations mapping algorithm [29], [30]. Since the information bearing signals are independent of each other within each group, the selected reference signals in these groups are independent of each other as well. As a result, for the total number of mapped bits carried by the specific indices of the selected reference signals, we have

$$m_1 = p_1 W = \lfloor \log_2 [C(N, U)] \rfloor W \tag{3}$$

where $C(N, U) = \frac{N!}{U!(N-U)!}$ is the combinatorial number and $\lfloor \cdot \rfloor$ means the floor function. On the other hand, since each group of information signals contains U information bearing signals and each information bearing signal can carry one M-ary constellation symbol, the overall number of modulated bits carried by all M-ary constellation symbols can be calculated as

$$m_2 = p_2 W = UnW \tag{4}$$

TABLE I
SYSTEM PARAMETERS AND THEIR MEANINGS

Parameters	Meanings
N	The number of reference chaotic signals
U	The number of selected reference chaotic signals
W	The number of groups of information bearing signals
M	The modulation order
m_1	The number of mapped bits per symbol
m_2	The number of modulated bits per symbol
m	The number of transmitted bits per symbol
n	The number of modulated bits carried by one M-ary constellation symbol
β	The length of chaotic sequence generated by chaotic signal generator

where $n = \log_2 M$ is the number of modulated bits carried by one M-ary constellation symbol and M denotes the modulation order, namely the number of constellation points. Accordingly, a total number of $m = m_1 + m_2 = (\lfloor \log_2 [C(N,U)] \rfloor + Un) W$ bits are transmitted by an MC-MOCVSK-IM symbol. The main system parameters are summarized in Table I. Considering an MC-MOCVSK-IM symbol, the transmitted signal of MC-MOCVSK-IM system is expressed as

$$s(t) = \sum_{k=N+1}^{N+W} \left[\frac{1}{\sqrt{U}} \sum_{u=1}^{U} \left(a_{k,u} x_{k,u}(t) + b_{k,u} y_{k,u}(t) \right) \times \cos(2\pi f_k t) \right] + \sum_{j=1}^{N} x_j(t) \cos(2\pi f_j t) \quad (5)$$

where $x_{k,u}(t)$ is the u^{th} information bearing signal in the k^{th} information subcarrier and $y_{k,u}(t) = \mathcal{H}(x_{k,u})$ is the orthogonal signal of $x_{k,u}(t)$, constructed by the Hilbert transform. $x_j(t)$ denotes reference signals in MC-MOCVSK-IM system. Note that information bearing signals $x_{k,u}(t), u = 1, 2, \cdots, U$ are selected from the reference signals $x_j(t), j = 1, 2, \cdots, N$ by k-combinations mapping algorithm. Then, $a_{k,u}$ and $b_{k,u}$ are real and imaginary parts of the M-ary constellation symbols corresponding to the u^{th} information bearing signal carried by the k^{th} information subcarrier. By multiplying the k^{th} group of information subcarriers by the coefficient $\frac{1}{\sqrt{U}}$, the overall energy of each group of information subcarriers is normalized to one. The frequency of k^{th} subcarrier is denoted by f_k.

B. The Receiver

Assuming that the transmitted signal $s(t)$ passes through the multipath Rayleigh fading channel with an additive white Gaussian noise where the channel coefficient of each path is deemed to be constant within the whole symbol period, the signal at the receiver is given by

$$r(t) = \sum_{l=1}^{L} \lambda_l (t - \zeta_l) \otimes s(t) + \eta(t) \quad (6)$$

where λ_l and ζ_l are propagation gain and channel delay of the l^{th} path, respectively. L denotes the number of paths, and $\otimes$ is the convolution operation. Then, $\eta(t)$ is a Gaussian white noise with zero mean and power spectral density of $\frac{N_0}{2}$.

The block diagram of MC-MOCVSK-IM receiver is drawn in Fig. 2. In order to extract the reference signals and W groups of information bearing signals from the received signal $r(t)$, we perform the manipulations as follows: First, the synchronous subcarriers are multiplied by the received signal $r(t)$ and thus the reference and information bearing signals are separated. Then, the resultant signals are filtered by matched filters. Finally, the outputs of matched filters are sampled with the time spacing $t = kT_c$.

In Fig. 2, each group of information bearing signals are independent of each other, therefore we focus on and analyse only the first group of information bearing signal here to make the problem more tractable. For each group, N possible decision variables corresponding to the in-phase and quadrature branches are obtained as

$$Z^a_{1,j} = \sum_{k=1}^{\beta} \left\{ \left(\sum_{l=1}^{L} \sum_{u=1}^{U} \frac{\lambda_l}{\sqrt{U}} \left(a_{1,u} x_{1,u,k-\tau_l} + b_{1,u} y_{1,u,k-\tau_l} \right) + \eta^I_k \right) \times \left(\sum_{l=1}^{L} \lambda_l x_{1,j,k-\tau_l} + \eta^R_k \right) \right\}, j = 1, 2, \cdots, N, \quad (7)$$

$$Z^b_{1,j} = \sum_{k=1}^{\beta} \left\{ \left(\sum_{l=1}^{L} \sum_{u=1}^{U} \frac{\lambda_l}{\sqrt{U}} \left(a_{1,u} x_{1,u,k-\tau_l} + b_{1,u} y_{1,u,k-\tau_l} \right) + \eta^I_k \right) \times \left(\sum_{l=1}^{L} \lambda_l y_{1,j,k-\tau_l} + \tilde{\eta}^R_k \right) \right\}, j = 1, 2, \cdots, N \quad (8)$$

where $Z^a_{1,j}$ and $Z^b_{1,j}$ are the possible decision variables of in-phase and quadrature branches corresponding to the j^{th} information bearing signal in the first group. $x_{1,u,k-\tau_l}$ denotes the $(k-\tau_l)^{th}$ sample of the u^{th} chaotic signal in the first group of information bearing signal and $y_{1,u,k-\tau_l}$ is orthogonal to $x_{1,u,k-\tau_l}$. Note that τ_l is the discretized value of the delay ζ_l given in (6). Then, η^R_k and η^I_k are the additive white Gaussian noise with zero mean and variance $\frac{N_0}{2}$, imposed on the reference and information bearing signals, respectively. Furthermore, $\tilde{\eta}^R_k$ passed by the Hilbert filter is orthogonal to η^R_k. Next, a linear combination of decision variables corresponding to the in-phase and quadrature branches is written as $Z_{1,j} = Z^a_{1,j} + \sqrt{-1} Z^b_{1,j}$, $j = 1, 2, \cdots, N$.

Let $\Omega = \{|Z_{1,1}|, |Z_{1,2}|, \cdots, |Z_{1,N}|\}$, then we obtain the U maximum out of set Ω, namely $\Omega' = \{|Z'_{1,1}|, |Z'_{1,2}|, \cdots, |Z'_{1,U}|\}$. The remaining part of Ω is $\Omega^* = \{|Z^*_{1,1}|, |Z^*_{1,2}|, \cdots, |Z^*_{1,N-U}|\}$. Thus, $\Omega = \Omega' \cup \Omega^*$. As a result, the U estimated indices are determined and then the mapped bits are restored by performing the opposite operation of k-combinations mapping algorithm [29], [30]. Once the specific indices have been determined, the demodulation process for the M-ary constellation symbols is straightforward. Here, the minimum distance decision criterion is applied to get the estimated u^{th} M-ary information symbol $\hat{\varepsilon}_u$ as

$$\hat{\varepsilon}_u = \arg\min_{\varepsilon \in S} \left(|Z'_{1,u} - \varepsilon|^2 \right), u = 1, 2, \cdots, U \quad (9)$$

where S denotes the all possible M-ary constellation points and ε is a possible point of M-ary constellation. Finally, by converting the estimated M-ary constellation symbols into a sequence of binary bits, the modulated bits are recovered successfully. Then the other groups of mapped bits as well as modulated bits can be retrieved using the procedure described above.

III. System Analysis

A. Energy Efficiency and Spectral Efficiency Comparisons

In this subsection, data-energy-to-bit-energy ratio (DBR), which denotes the ratio of data energy to bit energy, is used to evaluate the energy efficiency [17]. According to the configuration of MC-MOCVSK-IM system, N and W subcarriers are used to carry the reference and information bearing signals, respectively. There are $m = \lfloor \log_2 [C(N,U)] \rfloor W + UnW$

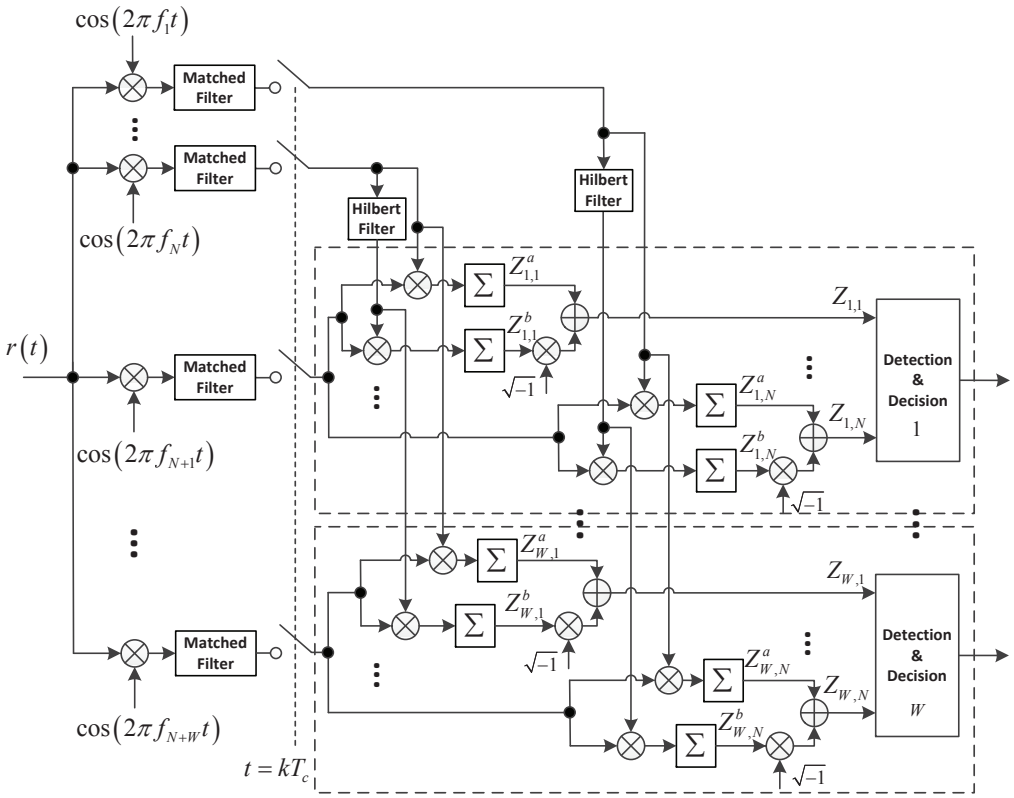

Fig. 2. The block diagram of MC-MOCVSK-IM receiver.

bits transmitted in an MC-MOCVSK-IM symbol where $m_1 = \lfloor \log_2 [C(N,U)] \rfloor W$ bits arranged for mapped bits and $m_2 = UnW$ are used for modulated bits. Therefore, the transmitted bit energy E_b is calculated as $E_b = \frac{(N+W)\sum_{k=1}^{\beta} x_{1,u,k-\tau_l}^2}{m}$. Similarly, the energy of data bearing signal E_{data} is equal to $E_{data} = W\sum_{k=1}^{\beta} x_{1,u,k-\tau_l}^2$. Consequently, the DBR of MC-MOCVSK-IM system is given as $DBR_1 = \frac{E_{data}}{E_b} = \frac{mW}{N+W}$.

Let assume that the total transmitted bits per symbol in MC-MOCVSK-IM, CI-DCSK and 2CI-DCSK systems are equal to m. The energy efficiency of CI-DCSK and 2CI-DCSK systems can be obtained as $DBR_2 = \frac{m}{2}$ and $DBR_3 = \frac{2m}{3}$, respectively. Table II shows the DBR values of MC-MOCVSK-IM, CI-DCSK and 2CI-DCSK systems. Note that a higher DBR value means more energy is used for data bearing signal, therefore a larger DBR is an indication of higher energy efficiency in non-coherent chaotic communication systems. Let $DBR_1 > DBR_3$, namely $\frac{mW}{N+W} > \frac{2m}{3}$, then $W > 2N$. Therefore, when the value of W is more than twice as much as N, MC-MOCVSK-IM system can achieve higher energy efficiency than CI-DCSK and 2CI-DCSK systems.

Spectral efficiency (SE) is defined as the ratio of bit rate to total bandwidth [22]. We assume that the bandwidth of each subcarrier equals to B and the overall number of transmitted bits per symbol in all systems are equal to m. Hence, the spectral efficiency of MC-MOCVSK-IM system is obtained as

$$SE_1 = \frac{\text{bit rate}}{\text{total bandwidth}} = \frac{m}{(N+W)\beta T_c B}. \tag{10}$$

Similarly, the spectral efficiency of CI-DCSK and 2CI-DCSK systems are given as $SE_2 = \frac{m}{(2^{m-1}+1)\beta T_c B}$ and $SE_3 = \frac{m}{\left(2^{\frac{m}{2}-1}+1\right)\beta T_c B}$, respectively. The spectral efficiency of MC-MOCVSK-IM, CI-DCSK and 2CI-DCSK systems are listed in Table II. When $SE_1 > SE_3$, namely $\frac{m}{(N+W)\beta T_c B} > \frac{m}{\left(2^{\frac{m}{2}-1}+1\right)\beta T_c B}$, we have $m > 2\log_2(N+W-1)+2$. In this case, the MC-MOCVSK-IM system can obtain higher spectral efficiency than CI-DCSK and 2CI-DCSK systems. Only one subcarrier is activated in CI-DCSK and two subcarriers are activated in 2CI-DCSK. Therefore, lots of subcarriers are not used for information transmission which results in great waste of subcarrier resource. In contrast, by using all subcarriers, MC-MOCVSK-IM system can achieve a higher spectral efficiency.

TABLE II
DBR AND SPECTRAL EFFICIENCY COMPARISONS OF MC-MOCVSK-IM, CI-DCSK AND 2CI-DCSK SYSTEMS

System	DBR	SE
MC-MOCVSK-IM	$\frac{mW}{N+W}$	$\frac{m}{(N+W)\beta T_c B}$
CI-DCSK	$\frac{m}{2}$	$\frac{m}{(2^{m-1}+1)\beta T_c B}$
2CI-DCSK	$\frac{2m}{3}$	$\frac{m}{\left(2^{\frac{m}{2}-1}+1\right)\beta T_c B}$

TABLE III
TRANSMITTER HARDWARE COMPLEXITY COMPARISON

System	MC-MOCVSK-IM	CI-DCSK	2CI-DCSK
Adder	$W+1$	1	$2^{\left(\frac{m}{2}-1\right)}+1$
Multipliers	$N+W$	2^m+1	$3\cdot 2^{\left(\frac{m}{2}-1\right)}+1$
Pulse shaping filter	N	1	2
Hilbert filter	UW	0	1
Modulator	M-ary DCSK modulator	DCSK modulator	DCSK modulator
Other blocks	Digital signal processor, k-combination mapper	Chaotic generator, Index selector	Chaotic generator, Index selector

TABLE IV
RECEIVER HARDWARE COMPLEXITY COMPARISON

System	MC-MOCVSK-IM	CI-DCSK	2CI-DCSK
Adder	$3NW$	0	0
Multipliers	$3NW+N+W$	$2^{m-1}+1$	$2^{\left(\frac{m}{2}-1\right)}+1$
Matched filter	$N+W$	$2^{m-1}+1$	$2^{\left(\frac{m}{2}-1\right)}+1$
Hilbert filter	N	0	1
Demodulator	M-ary DCSK demodulator	DCSK demodulator	DCSK demodulator
Other blocks	Index detection	Index detection	Index detection

B. Hardware Complexity Comparison

The components used to construct the transmitters and receivers of MC-MOCVSK-IM, CI-DCSK and 2CI-DCSK systems are given in Table III and Table IV, respectively. Assume that the total number of transmitted bits in MC-MOCVSK-IM, CI-DCSK and 2CI-DCSK systems is equal to m. As shown in Table III, in order to produce orthogonal and normalized chaotic signals, a complicated digital signal processor is necessary in the MC-MOCVSK-IM transmitter. Moreover, UW Hilbert filters and N pulse shaping filters are needed in the MC-MOCVSK-IM transmitter which greatly increases system complexity. Besides, since M-ary DCSK demodulator and many Hilbert filters are applied in the MC-MOCVSK-IM receiver, the receiver complexity of MC-MOCVSK-IM system is larger than that of the CI-DCSK and 2CI-DCSK systems. Therefore the hardware complexity of MC-MOCVSK-IM is much higher than that of its competitors. This higher complexity has to be used to get better energy and spectral efficiencies.

IV. PERFORMANCE ANALYSIS

In this section, we analyse the bit error probability of MC-MOCVSK-IM system for the cases of AWGN and multipath Rayleigh fading channels. In the following derivations, it is assumed that the largest path delay is far less than spreading factor, namely $0 < \tau_{\max} \ll \beta$, so that the inter-symbol interference arising from the multipath channel is negligible. Then on the condition of large spreading factor, it holds that

$$\sum_{k=1}^{\beta} x_{1,j,k-\tau_l} y_{1,u,k-\tau_l} \approx 0, \tag{11}$$

$$\sum_{k=1}^{\beta} x_{1,j,k-\tau_l} x_{1,u,k-\tau_l} \approx 0, j \neq u. \tag{12}$$

Accordingly, expanding (7) and (8) we obtain

$$\begin{aligned} Z_{1,j}^{a} \approx & \sum_{k=1}^{\beta}\sum_{l=1}^{L}\sum_{u=1}^{U} \frac{\lambda_l}{\sqrt{U}} \left(a_{1,u} x_{1,u,k-\tau_l} + b_{1,u} y_{1,u,k-\tau_l}\right)\eta_k^R \\ & + \sum_{k=1}^{\beta}\sum_{l=1}^{L}\sum_{u=1}^{U} \frac{\lambda_l^2}{\sqrt{U}} a_{1,u} x_{1,j,k-\tau_l} x_{1,u,k-\tau_l} \\ & + \sum_{k=1}^{\beta}\sum_{l=1}^{L} \lambda_l x_{1,j,k-\tau_l}\eta_k^I + \sum_{k=1}^{\beta} \eta_k^R \eta_k^I, \end{aligned} \tag{13}$$

$$\begin{aligned} Z_{1,j}^{b} \approx & \sum_{k=1}^{\beta}\sum_{l=1}^{L}\sum_{u=1}^{U} \frac{\lambda_l}{\sqrt{U}} \left(a_{1,u} x_{1,u,k-\tau_l} + b_{1,u} y_{1,u,k-\tau_l}\right)\tilde{\eta}_k^R \\ & + \sum_{k=1}^{\beta}\sum_{l=1}^{L}\sum_{u=1}^{U} \frac{\lambda_l^2}{\sqrt{U}} b_{1,u} y_{1,j,k-\tau_l} y_{1,u,k-\tau_l} \\ & + \sum_{k=1}^{\beta}\sum_{l=1}^{L} \lambda_l y_{1,j,k-\tau_l}\eta_k^I + \sum_{k=1}^{\beta} \tilde{\eta}_k^R \eta_k^I. \end{aligned} \tag{14}$$

Because the decision variables corresponding to in-phase and quadrature branches are mutually symmetric, we only need to evaluate one of them. Considering the orthogonal chaotic vectors in (1), the decision variable $Z_{1,j}^{a}$, for the case of correct index detection, i.e., $j \in \{1, 2, \cdots, U\}$, can be mathematically

formulated as

$$Z_{1,j}^{a} \approx \sum_{k=1}^{\beta}\sum_{l=1}^{L}\sum_{u=1}^{U}\frac{\lambda_l}{\sqrt{U}}\left(a_{1,j}x_{1,u,k-\tau_l}+b_{1,j}y_{1,u,k-\tau_l}\right)\eta_k^R + \sum_{k=1}^{\beta}\sum_{l=1}^{L}\frac{\lambda_l^2}{\sqrt{U}}a_{1,j}x_{1,j,k-\tau_l}^2 + \sum_{k=1}^{\beta}\sum_{l=1}^{L}\lambda_l x_{1,j,k-\tau_l}\eta_k^I + \sum_{k=1}^{\beta}\eta_k^R\eta_k^I. \quad (15)$$

When the index detection is wrong, i.e., $j \notin \{1,2,\cdots,U\}$, the decision variable $Z_{1,j}^{a}$ is

$$Z_{1,j}^{a} \approx \sum_{k=1}^{\beta}\sum_{l=1}^{L}\sum_{u=1}^{U}\frac{\lambda_l}{\sqrt{U}}\left(a_{1,u}x_{1,u,k-\tau_l}+b_{1,u}y_{1,u,k-\tau_l}\right)\eta_k^R + \sum_{k=1}^{\beta}\sum_{l=1}^{L}\lambda_l x_{1,j,k-\tau_l}\eta_k^I + \sum_{k=1}^{\beta}\eta_k^R\eta_k^I. \quad (16)$$

The symbol energy in the MC-MOCVSK-IM system is obtained as $E_s = (N+W)\sum_{k=1}^{\beta}x_{1,j,k-\tau_l}^2 = (N+W)\sum_{k=1}^{\beta}y_{1,j,k-\tau_l}^2$. The decision variable $Z_{1,j}^{a}$ can be characterized by a Gaussian distribution [11] with

$$\mathrm{E}\left[Z_{1,j}^{a}\right] = \begin{cases} \sum_{l=1}^{L}\lambda_l^2\frac{a_{1,j}E_s}{\sqrt{U}(N+W)}, & j\in\{1,2,\cdots,U\} \\ 0, & j\notin\{1,2,\cdots,U\} \end{cases} \quad (17)$$

$$\mathrm{Var}\left[Z_{1,j}^{a}\right] = \sum_{l=1}^{L}\lambda_l^2\frac{E_sN_0}{N+W}+\beta\frac{N_0^2}{4}=\sigma^2 \quad (18)$$

where $\mathrm{E}[\cdot]$ and $\mathrm{Var}[\cdot]$ denote the mean and variance operations, respectively. Similarly, the mean and variance of $Z_{1,j}^{b}$ are obtained as

$$\mathrm{E}\left[Z_{1,j}^{b}\right] = \begin{cases} \sum_{l=1}^{L}\lambda_l^2\frac{b_{1,j}E_s}{\sqrt{U}(N+W)}, & j\in\{1,2,\cdots,U\} \\ 0, & j\notin\{1,2,\cdots,U\} \end{cases} \quad (19)$$

$$\mathrm{Var}\left[Z_{1,j}^{b}\right] = \sum_{l=1}^{L}\lambda_l^2\frac{E_sN_0}{N+W}+\beta\frac{N_0^2}{4}=\sigma^2. \quad (20)$$

Since the decision variables of $Z_{1,j}^{a}$ and $Z_{1,j}^{b}$ are independent of each other, we get

$$\mathrm{E}[Z_{1,j}] = \mathrm{E}\left[Z_{1,j}^{a}\right]+\mathrm{E}\left[Z_{1,j}^{b}\right] = \begin{cases} \sum_{l=1}^{L}\lambda_l^2\frac{(a_{1,j}+b_{1,j})E_s}{\sqrt{U}(N+W)}=\mu_1, & j\in\{1,2,\cdots,U\} \\ 0, & j\notin\{1,2,\cdots,U\} \end{cases} \quad (21)$$

$$\mathrm{Var}[Z_{1,j}] = \mathrm{Var}\left[Z_{1,j}^{a}\right]+\mathrm{Var}\left[Z_{1,j}^{b}\right] = 2\left(\sum_{l=1}^{L}\lambda_l^2\frac{E_sN_0}{N+W}+\beta\frac{N_0^2}{4}\right)=\sigma_1^2. \quad (22)$$

As shown in Fig. 2, to get the indices of the selected reference signals, the detection and decision block is applied to find the U maximum absolute values $|Z'_{1,u}|$, $u=1,2,\cdots,U$ from the variables $|Z_{1,j}|, j=1,2,\cdots,N$. The remaining part of $|Z_{1,j}|, j=1,2,\cdots,N$ is given as $\left|Z_{1,i}^{*}\right|, i=1,2,\cdots,N-U$. Let $X = \min_{u=1,2,\cdots,U}(|Z'_{1,u}|)$ and $Y = \max_{i=1,2,\cdots,N-U}\left(\left|Z_{1,i}^{*}\right|\right)$. According to [29, eq.(14)], the probability for the incorrect index detection is obtained as

$$P_{id} = \int_{-\infty}^{+\infty}\left[1-\Pr\{X>Y\}\right]f_X(x)\,\mathrm{d}x \quad (23)$$

where $f_X(x)$ is the probability density function (PDF) of X.

The U random variables $\left|Z'_{1,u}\right|$, $u=1,2,\cdots,U$ are independent of each other and they have identical distribution. Consequently, the cumulative distribution function (CDF) of X is represented as

$$F_X(x) = 1-\left[1-F_{|Z'_{1,u}|}(x)\right]^{U}. \quad (24)$$

Subsequently, the PDF of X is deduced by executing the derivation of $F_X(x)$, i.e.,

$$f_X(x) = U\left[1-F_{|Z'_{1,u}|}(x)\right]^{U-1}f_{|Z'_{1,u}|}(x) \quad (25)$$

where $f_{|Z'_{1,u}|}(x)$ and $F_{|Z'_{1,u}|}(x)$ are the PDF and CDF of $\left|Z'_{1,u}\right|$ given by [32]

$$f_{|Z'_{1,u}|}(x) = \frac{1}{\sqrt{2\pi\sigma_1^2}}\left(e^{-\frac{(x-\mu_1)^2}{2\sigma_1^2}}+e^{-\frac{(x+\mu_1)^2}{2\sigma_1^2}}\right), \quad (26)$$

$$F_{|Z'_{1,u}|}(x) = \frac{1}{2}\left[\mathrm{erf}\left(\frac{(x-\mu_1)}{\sqrt{2\sigma_1^2}}\right)+\mathrm{erf}\left(\frac{(x+\mu_1)}{\sqrt{2\sigma_1^2}}\right)\right] \quad (27)$$

where $\mathrm{erf}(x)=\frac{2}{\sqrt{\pi}}\int_0^x e^{-t^2}\mathrm{d}t$ denotes the error function.

On the other hand, other decision variables $\left|Z_{1,i}^{*}\right|$, $i=1,2,\cdots,N-U$ are independent and identically distributed (i.i.d). Exploiting the properties of folded normal distribution [32], (23) can be simplified as

$$P_{id} = \int_{0}^{+\infty}\left[1-\left(F_{|Z_{1,i}^{*}|}(x)\right)^{N-U}\right]f_X(x)\mathrm{d}x \quad (28)$$

where $F_{|Z_{1,i}^{*}|}$ is the CDF of $\left|Z_{1,i}^{*}\right|$ given by

$$F_{|Z_{1,i}^{*}|} = \mathrm{erf}\left(\frac{x}{\sqrt{2\sigma_1^2}}\right) \quad (29)$$

Substituting (25) and (29) into (28) and exploiting the identity $\mathrm{erfc}(x)=1-\mathrm{erf}(x)$, the erroneous index detection probability is obtained as

$$P_{id} = \int_{0}^{+\infty}\frac{U}{\sqrt{2\pi\sigma_1^2}}\left(\frac{1}{2}\right)^{U-1}\left\{1-\left[\mathrm{erf}\left(\frac{x}{\sqrt{2\sigma_1^2}}\right)\right]^{N-U}\right\} \times\left[\mathrm{erfc}\left(\frac{(x-\mu_1)}{\sqrt{2\sigma_1^2}}\right)+\mathrm{erfc}\left(\frac{(x+\mu_1)}{\sqrt{2\sigma_1^2}}\right)\right]^{U-1} \times\left(e^{-\frac{(x-\mu_1)^2}{2\sigma_1^2}}+e^{-\frac{(x+\mu_1)^2}{2\sigma_1^2}}\right)\mathrm{d}x \quad (30)$$

where $\mathrm{erfc}(x)$ is the complementary error function, defined as $\mathrm{erfc}(x)=\frac{2}{\sqrt{\pi}}\int_x^{+\infty}e^{-t^2}\mathrm{d}t$.

When $M=2$, the M-ary modulation degrades into an

ordinary binary modulation and the quadrature branch vanishes, leaving the in-phase branch. In this case, the statistical parameters have a simpler form satisfying

$$\mathrm{E}\left[Z_{1,j}\right]=\begin{cases}\sum\limits_{l=1}^{L}\lambda_l^2\frac{E_s}{\sqrt{U}(N+W)}=\mu_2, & j\in\{1,2,\cdots,U\}\\ 0, & j\notin\{1,2,\cdots,U\}\end{cases} \tag{31}$$

$$\mathrm{Var}\left[Z_{1,j}\right]=\sum_{l=1}^{L}\lambda_l^2\frac{E_sN_0}{N+W}+\beta\frac{N_0^2}{4}=\sigma_2^2. \tag{32}$$

In particular, replacing μ_1 and σ_1^2 by μ_2 and σ_2^2 in (30), respectively, the erroneous index detection probability is obtained. Afterwards, according to [23], the relationship between erroneous index detection probability and the BER of mapped bits is obtained as

$$P_{map}=\frac{2^{p_1-1}}{2^{p_1}-1}P_{id}. \tag{33}$$

The previous parts have derived the bit error probability for mapped bits including the case of binary modulation and M-ary modulation. The bit error rate of modulated bits will be analyzed in the following parts. Especially, the incorrect detection of modulated bits are determined for two completely different cases. In the first case, it still has $\frac{1}{2}$ bit error rate for modulated bits on the condition of incorrect index detection. Therefore, it contributes parts of BER for modulated bits, interpreted as $P_1=\frac{1}{2}P_{id}$. With respect to the second case, when the index detection is carried out without taking along any errors, modulated bits are estimated incorrectly with the probability of [11, eq.(21)], [17, eq.(12)]

$$\begin{aligned}P_e\approx&\frac{1}{\log_2 M}\left[1-\int_{-\frac{\pi}{M}}^{\frac{\pi}{M}}\frac{1}{2\pi}\exp\left(-\frac{\rho^2}{2}\right)\right.\\&\left.+\exp\left(-\frac{\rho^2\sin^2 t}{2}\right)\frac{\rho\cos t}{\sqrt{2\pi}}Q\left(-\rho\cos t\right)\mathrm{d}t\right]\end{aligned} \tag{34}$$

where $Q(x)=\frac{1}{\sqrt{2\pi}}\int_x^{+\infty}\exp\left(-\frac{t^2}{2}\right)\mathrm{d}t$, $x\geq 0$, $\rho=\frac{E_m}{\sigma}$, $E_m=\sum\limits_{l=1}^{L}\lambda_l^2\frac{E_s}{\sqrt{U}(N+W)}$ and $\sigma^2=\sum\limits_{l=1}^{L}\lambda_l^2\frac{E_sN_0}{N+W}+\beta\frac{N_0^2}{4}$. Hence, after some manipulations, we get

$$\rho=\frac{E_m}{\sigma}=\frac{2\gamma_s}{\sqrt{4U\left(N+W\right)\gamma_s+\beta U(N+W)^2}} \tag{35}$$

where $\gamma_s=\sum\limits_{l=1}^{L}\lambda_l^2\frac{E_s}{N_0}$ denotes instantaneous symbol signal-to-noise ratio (SNR). Particularly, taking the binary modulation into consideration when $M=2$, the bit error probability for the modulated bits is obtained as

$$\begin{aligned}P_e=&\frac{1}{2}\mathrm{erfc}\left[\left(\frac{2\sigma_2^2}{\mu_2^2}\right)^{-\frac{1}{2}}\right]\\=&\frac{1}{2}\mathrm{erfc}\left[\left(\frac{2U\left(N+W\right)}{\gamma_s}+\frac{\beta U(N+W)^2}{2\gamma_s^2}\right)^{-\frac{1}{2}}\right].\end{aligned} \tag{36}$$

It is crucial to notice that the remaining error contribution for modulated bits, generated in the second case, is given as $P_2=P_e\left(1-P_{id}\right)$. Recalling the results of previous analysis, the overall bit error probability of modulated bits P_{mod} is the sum of P_1 and P_2, i.e.,

$$P_{mod}=P_e\left(1-P_{id}\right)+\frac{1}{2}P_{id}. \tag{37}$$

Therefore, for equiprobable transmission of information bits, the BER of MC-MOCVSK-IM system is given by

$$\begin{aligned}P_T=&\frac{m_1}{m_1+m_2}P_{map}+\frac{m_2}{m_1+m_2}P_{mod}\\=&\frac{p_1}{p_1+p_2}P_{map}+\frac{p_2}{p_1+p_2}P_{mod}.\end{aligned} \tag{38}$$

Considering the L-path disparate Rayleigh fading channel, the instantaneous symbol SNR γ_s possesses the probability density function of [17], [31]

$$f\left(\gamma_s\right)=\sum_{l=1}^{L}\left[\frac{1}{\bar{\gamma}_l}\left(\prod_{j=1,j\neq l}^{L}\frac{\bar{\gamma}_l}{\bar{\gamma}_l-\bar{\gamma}_j}\right)\exp\left(-\frac{\gamma_s}{\bar{\gamma}_l}\right)\right], \tag{39}$$

where $\bar{\gamma}_l$ is the average of instantaneous SNR $\gamma_l=\lambda_l^2\frac{E_s}{N_0}$ measured in the l^{th} channel. As a matter of fact, when each path of the L-path channel is independent and all of them satisfy the identical Rayleigh distribution, the PDF of instantaneous symbol SNR γ_s is given as

$$f\left(\gamma_s\right)=\frac{\gamma_s^{L-1}}{(L-1)!\bar{\gamma}_c^L}\exp\left(-\frac{\gamma_s}{\bar{\gamma}_c}\right) \tag{40}$$

where

$$\bar{\gamma}_c=\frac{E_s}{N_0}\mathrm{E}\left[\lambda_j^2\right]=\frac{E_s}{N_0}\mathrm{E}\left[\lambda_l^2\right],j\neq l. \tag{41}$$

Finally, the average bit error probability of the proposed MC-MOCVSK-IM system over multipath Rayleigh fading channel is obtained after evaluating the integral of

$$\bar{P}_T=\int_0^{+\infty}P_T\cdot f\left(\gamma_s\right)\mathrm{d}\gamma_s. \tag{42}$$

Substituting (38), (39) and/or (40) into (42), the BER of MC-MOCVSK-IM system over multipath Rayleigh fading channel can be obtained. In particular, when channel parameters are equal to $L=1$, $\lambda_1=1$ and $\tau_1=0$, the channel is degraded into the well-known AWGN channel.

V. Results and Discussions

In this section, the BER performance of MC-MOCVSK-IM system is evaluated over both AWGN and multipath Rayleigh fading channels by computer simulation for different system parameters. In addition, to highlight the superiority of MC-MOCVSK-IM system, the BER performance of MC-MOCVSK-IM system is compared with that of other non-coherent chaotic communication systems. Two different channel models are considered for multipath Rayleigh fading channel. The first channel model referred to as CM1 is a three-ray channel with the same channel coefficients $\mathrm{E}\left(\lambda_1^2\right)=\mathrm{E}\left(\lambda_2^2\right)=\mathrm{E}\left(\lambda_3^2\right)=\frac{1}{3}$. The second channel model referred to as CM2 is a three-ray channel with different channel coefficients $\mathrm{E}\left(\lambda_1^2\right)=\frac{1}{2}$, $\mathrm{E}\left(\lambda_2^2\right)=\frac{1}{3}$, $\mathrm{E}\left(\lambda_3^2\right)=\frac{1}{6}$. The path delays for both CM1 and CM2 are set to $\tau_1=0$, $\tau_2=T_c$, $\tau_3=2T_c$.

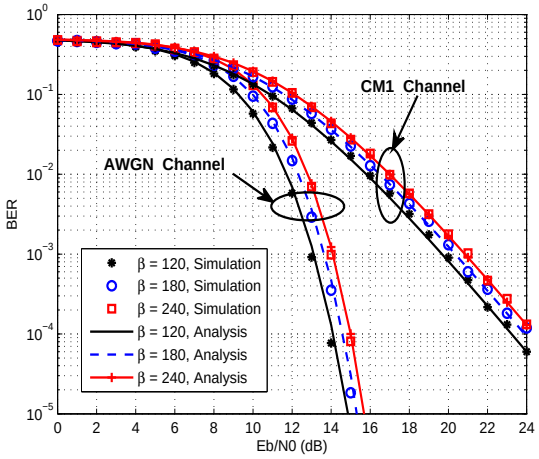

Fig. 3. BER performance of MC-MOCVSK-IM system with $N = 4$, $U = 1$, $W = 8$, $M = 2$ and $\beta = 120, 180, 240$ over AWGN and CM1 channels.

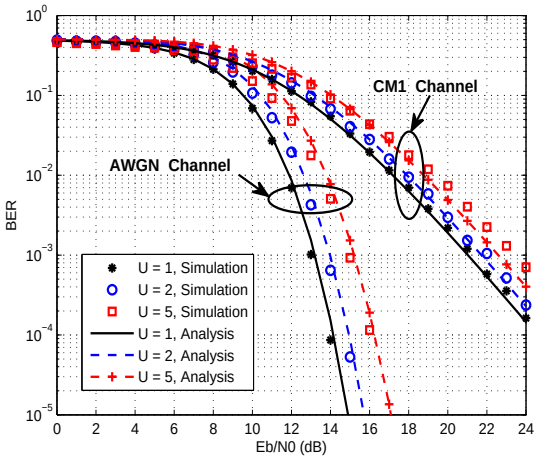

Fig. 4. BER performance of MC-MOCVSK-IM system with $N = 8$, $W = 8$, $M = 2$ and $U = 1, 2, 5$ over AWGN and CM1 channels.

A. Performance Evaluation under Various System Parameters

In this subsection, we investigate the influence of different system parameters on the BER performance of MC-MOCVSK-IM system for the case of AWGN and CM1 channels. As the most basic parameter of a spread-spectrum system, the effect of spreading factor β on the BER performance of MC-MOCVSK-IM system is evaluated at first. As clearly shown in Fig. 3, when the spreading factor increases, the BER performance of MC-MOCVSK-IM system deteriorates over both channels. This is due to that when the value of spreading factor is increased, more noise components are received. Moreover, Fig. 3 also shows a good match between the simulation and analytical results, providing a proof for our theoretical derivations in the previous section.

In order to explore the effect of parameter U on BER performance, we have simulated the MC-MOCVSK-IM system over AWGN and CM1 channels with $N = 8$, $W = 8$, $M = 2$ and $U = 1, 2, 5$, respectively. As illustrated in Fig. 4, the theoretical results are in an excellent agreement with the simulation results. The MC-MOCVSK-IM system shows a decline in BER performance when the value of U is increased. From the perspective of simulation parameters above, it concludes that the number of mapped bits is calculated as $p_1 = 3, 4, 5$ within single group of information bearing signal in the case of $U = 1, 2, 5$, while the number of modulated bits is given as $p_2 = 1, 2, 5$, respectively. Although more mapped bits are conveyed with larger U which should result in a better BER performance, the proportion of mapped bits to modulated bits shows a declining trend which restrains the performance improvement. A larger U means that more information bearing signals are involved within the same information subcarrier and thus the interference in index detection gets more severe and causes a worse BER performance.

Fig. 5 shows the BER performance of MC-MOCVSK-IM system for diverse W and M over AWGN and CM1 channels, respectively. As expected, in AWGN channel, the MC-MOCVSK-IM system with $W = 2$ and $M = 2$ offers about 1dB performance gain over $W = 2$ and $M = 8$ at

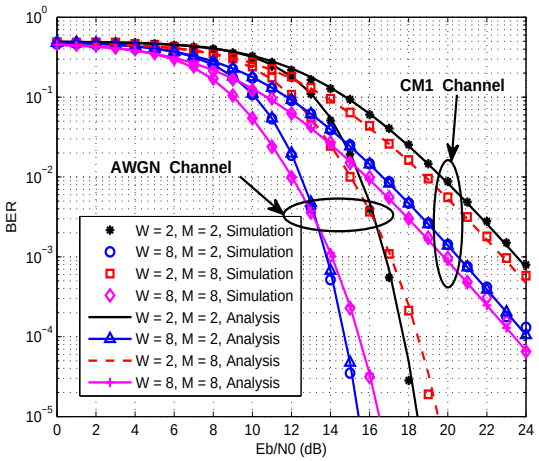

Fig. 5. BER performance of MC-MOCVSK-IM system with $\beta = 200$, $N = 4$, $U = 1$, $W = 2, 8$ and $M = 2, 8$ over AWGN and CM1 channels.

BER level of 10^{-5}. This is due to the fact that a larger modulation order results in the denser constellation points, thereby the distance between adjacent constellation points will be shorter, resulting in higher bit error rate. When M is fixed, e.g. $M = 2$, the performance improvement of MC-MOCVSK-IM with $W = 8$ over $W = 2$ is almost 3dB, which seems to be surprising but reasonable. In terms of single group of information bearing signal, the number of mapped bits and modulated bits remain unchanged, i.e., $p_1 = 2$ and $p_2 = 1$. However, the overall number of mapped bits and modulated bits within all information bearing signals is increased. $p_1 W = 4$ and $p_2 W = 2$ when $W = 2$, while $p_1 W = 16$ and $p_2 W = 8$ when $W = 8$. In other words, more mapped bits will be conveyed in an MC-MOCVSK-IM symbol on the condition of same transmitted energy, therefore the required SNR to reach certain BER is decreased.

Fig. 6 shows the BER performances of MC-MOCVSK-IM system over AWGN and CM1 channels with $N = 4$, $U = 1$, $W = 8$, $M = 2, 8$ and various spreading factors. Simulation

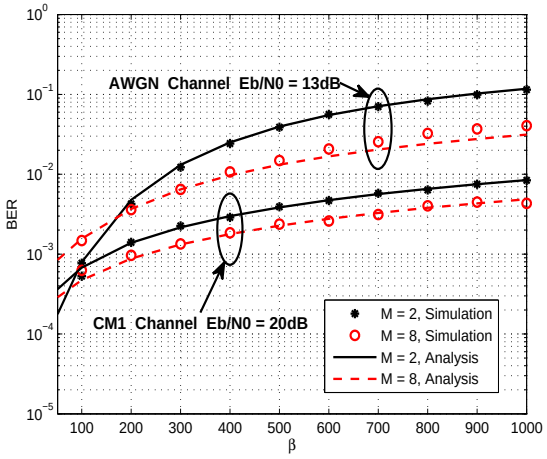

Fig. 6. The joint influence of β and M on the BER performance of MC-MOCVSK-IM system with $N = 4$, $U = 1$, $W = 8$, $M = 2, 8$ and various spreading factors over AWGN and CM1 channels.

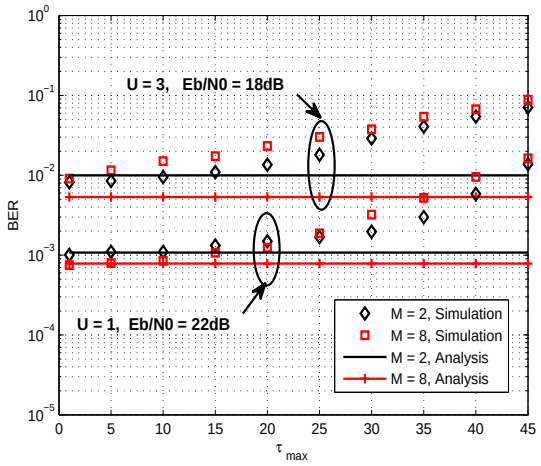

Fig. 7. The joint influence of U, M and $\tau_{\max}$ on the BER performance of MC-MOCVSK-IM system with $\beta = 100$, $N = 4$ and $W = 16$ over a two-path Rayleigh fading channel.

results match the theoretical results well, therefore the validity of our derivations is confirmed. When the spreading factor increases, the BER performance of MC-MOCVSK-IM system is deteriorated in both AWGN and CM1 channels. In AWGN channel, the slope of curve with $M = 2$ is larger than that of $M = 8$ in the scope of first halve of horizontal axis, which demonstrates MC-MOCVSK-IM system with $M = 2$ is more sensitive to noise. Note that the curve slope of $M = 2$ is quite approximate to that of $M = 8$ in the range of $\beta = [500, 1000]$. Regarding to the case of CM1 channel, the curves with $M = 2$ and $M = 8$ show rising tendency with similar slopes.

As a matter of fact, the impact of inter-symbol interference is ignored in our analysis by virtue of the widely used hypotheses of $\beta \gg \tau_{\max}$. Fig. 7 shows the effect of the inter-symbol interference on the performance of MC-MOCVSK-IM system. A two-path Rayleigh fading channel with the equal gain coefficients $\mathrm{E}\left(\lambda_1^2\right) = \mathrm{E}\left(\lambda_2^2\right) = \frac{1}{2}$ and different maximum path delays $\tau_{\max}$ is applied in our simulation. Clearly, simulation results match the analytical results when the maximum path delay is relatively small. The simulation performance of MC-MOCVSK-IM system gets worse and worse with the increasing of $\tau_{\max}$, whereas the theoretical BER remains constant. This suggests more crucial effect of path delay is involved in the BER performance of MC-MOCVSK-IM system when a larger path delay is considered.

B. BER Performance Comparison with Other Chaotic Communication Systems

To show the excellent BER performance of MC-MOCVSK-IM system, the performance comparison of MC-MOCVSK-IM, MC-CSK and MC-DCSK system is performed on the condition of same number of subcarriers N_s over AWGN and CM2 channels. The comparison results are given in Fig. 8. When $N_s = 64$, we have simulated the MC-MOCVSK-IM system with $N = 16$, $U = 1$, $W = 48$ and $M = 2$. In MC-CSK system, the number of reference subcarriers M_c is set to 64. Apparently, MC-MOCVSK-IM system achieves

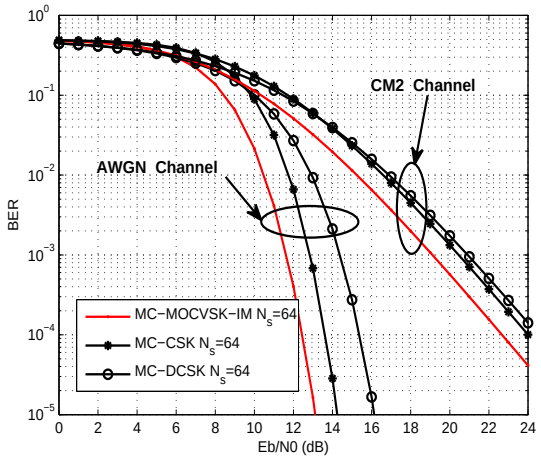

Fig. 8. BER performance comparison of MC-MOCVSK-IM, MC-CSK and MC-DCSK systems on the condition of same number of subcarriers $N_s = 64$ and $\beta = 200$ over AWGN and CM2 channels.

the best BER performance compared to its competitors. For example, in AWGN channel, the performance improvement of MC-MOCVSK-IM system over MC-CSK system exceeds 1dB at the BER of 10^{-5}. As for CM2 channel, the performance gain between MC-MOCVSK-IM and MC-CSK is almost 2dB at 10^{-4} BER level.

In Fig. 9, we compare the BER performance of MC-MOCVSK-IM with MC-CSK and MC-DCSK systems in the case of the same number of transmitted bits per symbol, i.e., $N_t = 64$. MC-MOCVSK-IM system uses the parameters $N = 8$, $U = 1$, $W = 16$ and $M = 2$ for its simulation. As observed in Fig. 9, it demonstrates that MC-MOCVSK-IM system performs over 1.5dB better than MC-CSK system at the BER level 10^{-5} in AWGN channel. In CM2 channel, the performance gain of MC-MOCVSK-IM over MC-DCSK is about 1dB at the BER 10^{-4}.

In addition, the BER performance comparison of MC-MOCVSK-IM and other state-of-the-art non-coherent multi-

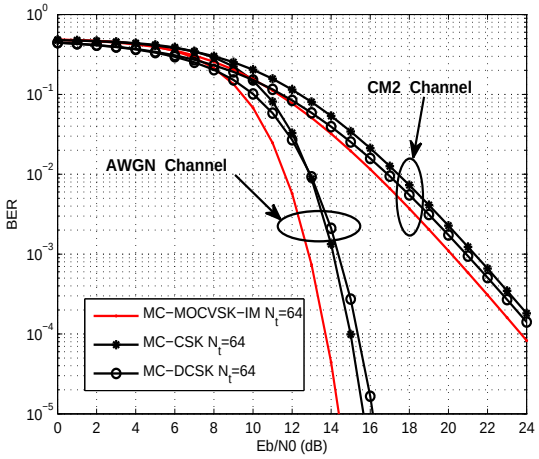

Fig. 9. BER performance comparison of MC-MOCVSK-IM, MC-CSK and MC-DCSK systems on the condition of same number of transmitted bits per symbol $N_t = 64$ and $\beta = 200$ over AWGN and CM2 channels.

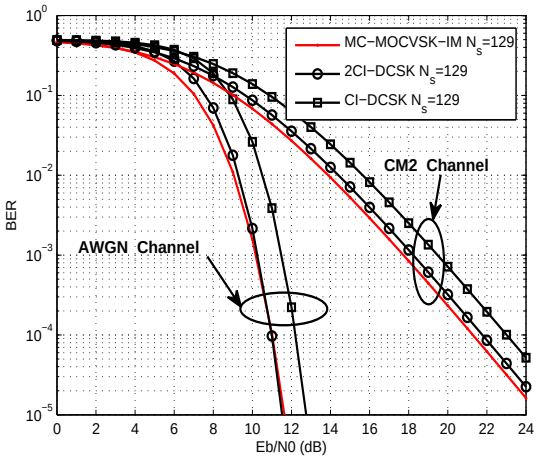

Fig. 10. BER performance comparison of MC-MOCVSK-IM and other state-of-the-art non-coherent multicarrier index chaotic communication system with constant number of carriers $N_s = 129$ and $\beta = 200$ over AWGN and CM2 channels.

carrier index chaotic communication system with same number of subcarriers $N_s = 129$ is performed in Fig. 10. MC-MOCVSK-IM system and its counterparts, i.e., 2CI-DCSK and CI-DCSK, have the similar transmission structure, namely all of them are equipped with the benefit of multicarrier modulation and index modulation. Hence this comparison is reasonable. In our simulation, $N = 16$, $U = 1$, $W = 113$ and $M = 4$ is used for MC-MOCVSK-IM system. As shown in Fig. 10, compared to 2CI-DCSK and CI-DCSK systems, MC-MOCVSK-IM system shows preferable robustness, especially in CM2 channel. Both 2CI-DCSK and CI-DCSK systems do not obtain the benefit of multicarrier modulation adequately because a mass of subcarriers are inactive. However, MC-MOCVSK-IM system takes full advantage of all subcarriers at the most extent and thus provides a higher data rate without sacrificing its BER performance and wasting subcarrier resources.

Finally, the BER performance of MC-MOCVSK-IM system is compared with CIM-MC-M-DCSK system in the case of same number of the transmitted bits per symbol, e.g., $N_t = 36$ and $N_t = 52$. Note that CM2 channel is used as multipath Rayleigh fading channel. The spreading factor is set to $\beta = 128$ in our simulation. When $N_t = 36$, the parameters $N = 4$, $U = 1$, $W = 9$ and $M = 4$ are adopted in MC-MOCVSK-IM simulation. In CIM-MC-M-DCSK system, the order of Walsh code is $N_o = 16$ and the order of M-ary modulation is $M = 4$. In regard to $N_t = 52$, MC-MOCVSK-IM uses $N = 2$, $U = 1$, $W = 13$ and $M = 8$ in its simulation. $N_o = 16$ and $M = 8$ are applied in CIM-MC-M-DCSK system. As shown in Fig. 11, the BER performance improvement of MC-MOCVSK-IM over CIM-MC-M-DCSK is about 3dB at BER level 10^{-5} in AWGN channel. When $N_t = 52$, the performance gain of MC-MOCVSK-IM over CIM-MC-M-DCSK is almost 3dB at BER level 10^{-3} in CM2 channel.

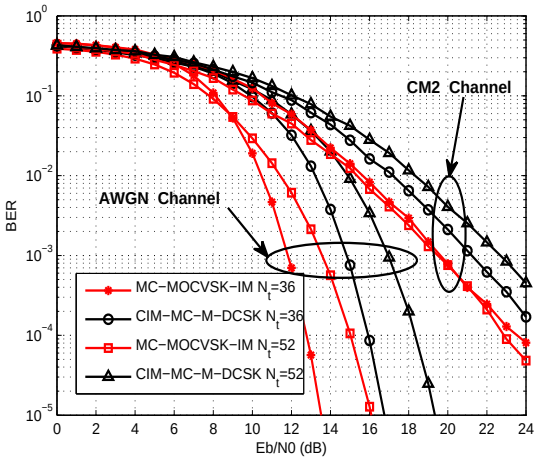

Fig. 11. BER performance comparison of MC-MOCVSK-IM and CIM-MC-M-DCSK with the same number of transmitted bits per symbol and $\beta = 128$ over AWGN and CM2 channels.

VI. Conclusions

A new multicarrier M-ary orthogonal chaotic vector shift keying with index modulation referred to as MC-MOCVSK-IM has been proposed in this paper, where the information bits are transmitted not only by the multiple groups of M-ary information bearing signals, but also by the specific indices of the selected reference signals. Exploiting and combining the benefits of OCVSK, multicarrier modulation, M-ary modulation and index modulation, MC-MOCVSK-IM system with the limited subcarrier resource can offer a higher data rate than other chaotic communication systems. The energy efficiency, spectral efficiency and system complexity of MC-MOCVSK-IM system have been compared to those of CI-DCSK and 2CI-DCSK systems. The comparison results show that MC-MOCVSK-IM system with appropriate parameters is capable to obtain higher energy and spectral efficiencies than its competitors at the expense of a bit higher system

complexity.

In addition, we have derived the theoretical BER expressions for MC-MOCVSK-IM system over AWGN and multipath Rayleigh fading channels. The analytical results have been verified by computer simulations. The BER performance comparison of MC-MOCVSK-IM system and the other non-coherent chaotic communication systems has been carried out. The comparison results demonstrate that the new MC-MOCVSK-IM system offers superior BER performance especially in the high-data-rate scenarios. Considering the massive demand for high-throughput and reliable wireless communication system, MC-MOCVSK-IM scheme is a great candidate for high-data-rate non-coherent chaotic communications.

REFERENCES

[1] T. Hwang, C. Yang, G. Wu, S. Li and G. Y. Li, "OFDM and its wireless applications: A survey," *IEEE Trans. Veh. Tech.*, vol. 58, no. 4, pp. 1673-1694, May 2009.

[2] A. Sahin, I. Guvenc and H. Arslan, "A survey on multicarrier communications: Prototype filters, lattice structures, and implementation aspects," *IEEE Commun. Surveys Tuts.*, vol. 16, no. 3, pp. 1312-1338, Third Quarter 2014.

[3] R. L. Devaney, *A First Course in Chaotic Dynamical Systems: Theory and Experiment*. Reading, MA, USA: Addison-Wesley, 1992.

[4] F. C. M. Lau and C. K. Tse, *Chaos-Based Digital Communication Systems*. Berlin, Germany: Springer-Verlag, 2003.

[5] G. Heidari-Bateni and C. McGillem, "Chaotic sequences for spread spectrum: an alternative to PN-sequences," *Proc. IEEE Int. Conf. Sel. Topics Wireless Commun.*, Jun. 1992, pp. 437C440.

[6] G. Kolumbán B. Vizvari, W. Schwarz, and A. Abel, "Differential chaos shift keying: A robust coding for chaotic communication," *Proc. Int. Workshop Nonlinear Dynam. Electron. Syst. (NDES)*, Jun. 1996, pp. 87C92.

[7] G. Kaddoum, "Wireless chaos-based communication systems: A comprehensive survey," *IEEE Access*, vol. 4, pp. 2621-2648, 2016.

[8] Y. Fang, G. Han, P. Chen, F. C. M. Lau, G. Chen and L. Wang, "A survey on DCSK-based communication systems and their application to UWB scenarios," *IEEE Commun. Surveys Tuts.*, vol. 18, no. 3, pp. 1804-1837, third quarter 2016.

[9] M. Dawa, G. Kaddoum and Z. Sattar, "A generalized lower bound on the bit error rate of DCSK systems over multi-path Rayleigh fading channels," *IEEE Trans. Circuits Syst. II, Exp. Briefs*, vol. 65, no. 3, pp. 321-325, March 2018.

[10] Z. Galias and G. M. Maggio, "Quadrature chaos-shift keying: Theory and performance analysis," *IEEE Trans. Circuits Syst. I, Reg. Papers*, vol. 48, no. 12, pp. 1510C1519, Dec. 2001.

[11] L. Wang, G. Cai and G. R. Chen, "Design and performance analysis of a new multiresolution M-ary differential chaos shift keying communication system," *IEEE Trans. Wireless Commun.*, vol. 14, no. 9, pp. 5197-5208, Sept. 2015.

[12] W. Xu, L. Wang, and G. Kolumbán, "A new data rate adaption communications scheme for code-shifted differential chaos shift keying modulation," *Int. J. Bifurcation Chaos*, vol. 22, no. 8, pp. 1-8, 2012.

[13] W. Xu, L. Wang, and G. Kolumbán, "A novel differential chaos shift keying modulation scheme," *Int. J. Bifurcation Chaos*, vol. 21, no. 3, pp. 799-814, 2011.

[14] G. Kaddoum and F. Gagnon, "Design of a high-data-rate differential chaos-shift keying system," *IEEE Trans. Circuits Syst. II, Exp. Briefs*, vol. 59, no. 7, pp. 448-452, Jul. 2012.

[15] T. Huang, L. Wang, W. Xu, and F. C. M. Lau, "Multilevel code-shifted differential-chaos-shift-keying system," *IET Commun.*, vol. 10, no. 10, pp. 1189-1195, 2016.

[16] X. Cai, W. Xu, R. Zhang and L. Wang, "A multilevel code shifted differential chaos shift keying system with M-ary modulation," *IEEE Trans. Circuits Syst. II, Exp. Briefs.*, vol. 66, no. 8, pp. 1451-1455, Aug. 2019.

[17] G. Kaddoum, F. Richardson, F. Gagnon, "Design and analysis of a multicarrier differential chaos shift keying communication system," *IEEE Trans. Commun.*, vol. 61, no. 8, pp. 3281-3291, Aug. 2013.

[18] G. Kaddoum, "Design and performance analysis of a multiuser OFDM based differential chaos shift keying communication system," *IEEE Trans. Commun.*, vol. 64, no. 1, pp. 249-260, Jan. 2016.

[19] E. Basar, M. Wen, R. Mesleh, M. Di Renzo, Y. Xiao and H. Haas, "Index modulation techniques for next-generation wireless networks," *IEEE Access*, vol. 5, pp. 16693-16746, 2017.

[20] G. Cheng, L. Wang, W. Xu and G. Chen, "Carrier Index Differential Chaos Shift Keying Modulation," *IEEE Trans. Circuits Syst. II, Exp. Briefs*, vol. 64, no. 8, pp. 907-911, Aug. 2017.

[21] G. Cheng, L. Wang, Q. Chen and G. Chen, "Design and performance analysis of generalised carrier index M-ary differential chaos shift keying modulation," *IET Commun.*, vol. 12, no. 11, pp. 1324-1331, 17 7 2018.

[22] W. Dai, H. Yang, Y. Song and G. Jiang, "Two-layer carrier index modulation scheme based on differential chaos shift keying," *IEEE Access*, vol. 6, pp. 56433-56444, 2018.

[23] X. Cai, W. Xu, L. Wang and F. Xu, "Design and performance analysis of differential chaos shift keying system with dual-index modulation," *IEEE Access*, vol. 7, pp. 26867-26880, 2019.

[24] G. Cai, Y. Fang, J. Wen, S. Mumtaz, Y. Song and V. Frascolla, "Multi-carrier M-ary DCSK system with code index modulation: An efficient solution for chaotic communications," *IEEE J. Sel. Areas Commun.*, doi: 10.1109/JSTSP.2019.2913944.

[25] T. J. Wren and T. C. Yang, "Orthogonal chaotic vector shift keying in digital communications," *IET Commun.*, vol. 4, no. 6, pp. 739-753, 16 April 2010.

[26] F. S. Hasan and A. A. Valenzuela, "Design and analysis of an OFDM-based orthogonal chaotic vector shift keying communication system," *IEEE Access*, vol. 6, pp. 46322-46333, 2018.

[27] H. Yang, W. K. S. Tang, G. Chen and G. Jiang, "Multi-carrier chaos shift keying: System design and performance analysis," *IEEE Trans. Circuits Syst. I, Reg. Papers*, vol. 64, no. 8, pp. 2182-2194, Aug. 2017.

[28] R. C. Chang, C. Lin, K. Lin, C. Huang and F. Chen, "Iterative QR decomposition architecture using the modified GramCSchmidt algorithm for MIMO systems," *IEEE Trans. Circuits Syst. I, Reg. Papers*, vol. 57, no. 5, pp. 1095-1102, May 2010.

[29] W. Xu, T. Huang and L. Wang, "Code-shifted differential chaos shift keying with code index modulation for high data rate transmission," *IEEE Trans. Commun.*, vol. 65, no. 10, pp. 4285-4294, Oct. 2017.

[30] E. Başar, Ü. Aygölü, E. Panayırcı and H. V. Poor, "Orthogonal frequency division multiplexing with index modulation," *IEEE Trans Signal Process.*, vol. 61, no. 22, pp. 5536-5549, Nov.15, 2013.

[31] J. G. Proakis and M. Salehi, *Digital Communications*. New York, NY, USA: McGraw-Hill, 2007.

[32] A. Papoulis, *Probability, Random Variables, and Stochastic Processes*. New York, NY, USA: McGraw-Hill, 1991.

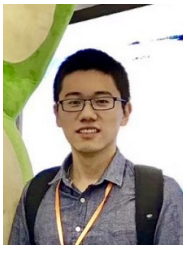

Xiangming Cai received the B.Sc. degree in information engineering from Guangdong University of Technology, Guangzhou, China, in 2017. He is currently pursuing the M.Sc. degree in the Department of Information and Communication Engineering, Xiamen University, Fujian, China. His research interests include chaos-based digital communications and their applications to wireless communications.

Weikai Xu (S'10-M'12) received the B.S. degree in electronic engineering from Three Gorges College, Chongqing, China, in 2000, the M.Sc. degree in communication and information system from the Chongqing University of Posts and Telecommunications, Chongqing, China, in 2003, and the Ph.D. degree in electronic circuit and system from the Xiamen University of China, Xiamen, China, in 2011. From 2003 to 2012, he was a Teaching Assistant, and Assistant Professor in Communication Engineering of Xiamen University. He is now an Associate Professor in Information and Communication Engineering of Xiamen University. His research interests include chaotic communications, underwater acoustic communications, channel coding, cooperative communications and ultra-wideband.

Lin Wang (S'99-M'03-SM'09) received the M.Sc. degree in applied mathematics from the Kunming University of Technology, China, in 1988, and the Ph.D. degree in electronics engineering from the University of Electronic Science and Technology of China, China, in 2001. From 1984 to 1986, he was a Teaching Assistant with the Mathematics Department, Chongqing Normal University. From 1989 to 2002, he was a Teaching Assistant, a Lecturer, and then an Associate Professor in applied mathematics and communication engineering with the Chongqing University of Post and Telecommunication, China. From 1995 to 1996, he was with the Mathematics Department, University of New England, Armidale, NSW, Australia, for one year. In 2003, he was a Visiting Researcher with the Center for Chaos and Complexity Networks, Department of Electronic Engineering, City University of Hong Kong, for three months. In 2013, he was a Senior Visiting Researcher with the Department of ECE, University of California at Davis, Davis, CA, USA. From 2003 to 2012, he was a Full Professor and an Associate Dean with the School of Information Science and Engineering, Xiamen University, China. He has been a Distinguished Professor since 2012. He holds 14 patents in the field of physical layer in digital communications. He has authored over 100 journal and conference papers. His current research interests are in the area of channel coding, joint source and channel coding, chaos modulation, and their applications to wireless communication and storage systems.

Géza Kolumbán Fellow of IEEE (2005), IEEE CAS Distinguished Lecturer (2013-2014), was graduated from and received his Ph.D. at the Technical University of Budapest and received his C.Sc. and D.Sc. degrees from the Hungarian Academy of Sciences. He spent 15 years in the telecommunications industry where he developed microwave circuits, PLL-based frequency synthesizers and was involved in many system engineering projects from satellite telecommunications to microwave digital radio systems. After joining the university education he showed that chaos may exist in autonomous PLLs and established noncoherent chaotic communications as a brand new research direction. He developed DCSK and FM-DCSK, the most popular chaotic modulation schemes. Two of his papers, written on chaos-based communications, have been ranked in the topcited IEEE Trans. CAS-I articles. He elaborated a unified theory for the Software Defined Electronics (SDE) systems and received the ICT Express's Best Paper Award in 2017 for the SDE concept. He has been a visiting professor and researcher to UC Berkeley, PolyU and CityU in Hong Kong, University College Dublin and Cork, Ireland, EPFL, Lausanne, Switzerland, INSA-LATTIS Laboratory, Toulouse, France, TU Dresden, Germany, Beijing Jiaotong University, China. Prof. Kolumbán has been providing consulting service for many companies from Samsung Advanced Institute of Technology to National Instruments. He is a full professor at the Pázmány Péter Catholic University, Budapest, Hungary and is an Adjunct Prof. at the Edith Cowan University, Perth, Australia. He served/is serving as an Associate Editor at IEEE TCAS-II, ICT Express, Elsevier DSP and Dynamics of Continuous, Discrete and Impulsive Systems, Series B.